

# Observation of Creep Following $K_0$ Consolidation of Loose Silty Sand

Muhamad Yusa

*University of Riau, Indonesia*

Elisabeth T. Bowman

*University of Sheffield, UK*

Misko Cubrinovski

*University of Canterbury, New Zealand*

## ABSTRAK:

Penelitian ini menyelidiki perilaku rangkak tanah pasir berlanau non-plastis (kadar butir halus 15%) dengan tingkat kepadatan lepas melalui triaksial tes dengan pengukuran langsung dibenda uji. Sample mula mula dikonsolidasi dengan regangan lateral dikekang pada tegangan penyekap 30, 60 dan 120 kPa, kemudian dibiarkan selama satu minggu dengan tegangan penyekap, deviator dan belakang dijaga konstan. Hasil pengukuran langsung pada benda uji dengan lokal axial dan radial transducer menunjukkan bahwa selama rangkak, semua benda uji berperilaku kontraktif. Regangan volumetrik benda uji dengan tegangan penyekap lebih tinggi lebih besar dari benda uji dengan tegangan penyekap lebih rendah.

This research investigated creep behavior of loose non-plastic (15% fine content) silty sand via triaxial testing using on-specimen measurement. Following  $K_0$  consolidation at 30, 60 and 120 kPa confining pressure, the samples were aged for one week at constant confining pressure, deviatoric stress and back pressure. The results from on-specimen measurements show that during creep, all the samples are contractive. Volumetric strains are greater for high confining pressures than for lower confining pressures

**Kata Kunci:** Rangkak, Triaksial,  $K_0$  konsolidasi, pasir berlanau, lepas

## 1 PENDAHULUAN - INTRODUCTION

It is well acknowledged that soil exhibit creep behavior, in which the deformation of soils develops with time under constant effective stress. Creep is significance for example, in the long term response of soils. Creep is also believed to be the one of the mechanisms of sand aging (Bowman, 2002; Mitchell, 2008; Schmertmann, 1991). Granular soil aging is particularly important to the development of stiffness and strength in shallow soils after artificial deposition or disturbance (e.g. hydraulic fills, vibrocompacted and blast densified soils) and post seismic liquefaction.

The field condition under which such soils age may be most closely approximated by  $K_0$  – i.e. where the lateral (horizontal ground) strain is zero while relatively low overburden stresses are applied. In spite of this, the

majority of studies on soil aging have been conducted under isotropic aging conditions (e.g. Bowman, 2002; Howie *et al.*, 2002; Mitchell, 2008; Schmertmann, 1991; Wang & Tsui, 2009). Kang *et al.* (2012) suggested that the application of shear during creep may serve to increase aging effects in denser soils by inducing a degree of dilation and interlocking of particles via void growth, although the degree to which shear is applied should not be so great as to induce creep rupture.  $K_0$  is an inherently stable condition in which, for normally deposited soil, the vertical effective stress is greater than the horizontal effective stress, resulting in a macroscopic deviatoric stress being applied.

Fine silty silica sand, with 15% non-plastic fines, was chosen as a test material because, although there have been a number of previous laboratory studies on sand aging, these have all

been conducted on clean sands (e.g. Kuwano & Jardine, 2002; Lade, 1994; Wang & Tsui, 2009). Natural sands are rarely “clean” and typically contain a proportion of fines which results in greater numbers of particle contacts and options for grain arrangement (fabric) and rearrangement. Hence it is expected that results from this study may be more applicable to the field condition in which non-clean sands dominate.

To summarize, this study reported observation of creep behavior of loose silty sand via triaxial test under different confining pressures.

## 2 EXPERIMENTAL PROGRAM

### 2.1 Material

The material used in this research program is fine silty sand. Silty sand was reconstituted in the laboratory by mixing sand and fine fractions ( $<75\mu\text{m}$ ). The sand fraction was collected from a site that liquefied during the Canterbury Earthquake, Christchurch, New Zealand in 2010 (Cubrinovski, 2013; Taylor *et al.*, 2012). Sand particle diameters range from  $75\mu\text{m}$  to  $300\mu\text{m}$ . The fine fraction is non-plastic silica flour with diameter range from  $32\mu\text{m}$  to  $75\mu\text{m}$ . The percentage of fine fraction used in this study is 15%. The specific gravity  $G_s$  for the sand and silt are 2.64 and 2.65, respectively. Maximum and minimum void ratios of the combined silty sand are 0.973 and 0.565, respectively. Figure 1 shows the particle size distribution of the combined soils.

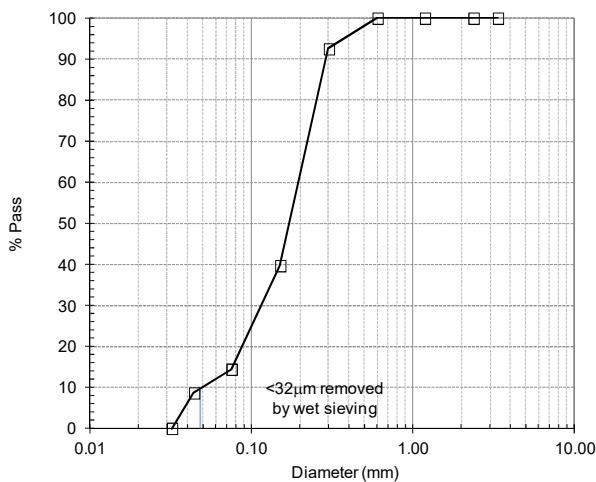


Fig. 1 Particle size distribution

### 2.2 Apparatus

Triaxial tests were conducted using a Geotechnical Digital System (GDS) triaxial machine that has been enhanced by adding a local on-sample strain measurement system, with one radial submersible Linear Variable Differential Transformer, LVDT, held by a radial strain belt, and two axial LVDTs, placed on either side of the sample.

The magnitude of axial strain during aging was expected to be in the order of 0.1% Shozen (2001) thus the local LVDT needed to be able to read less than 0.01%. This strain is equal to a resolution of about 0.0065mm (the gauge length between the upper axial pad and lower axial pad being about 65 mm). The minimum required analogue to digital converter (ADC) bit resolution is calculated from equation below

$$resolution = \{\log[(V_d E)/(R V_s)] / \log(2)\} + B \quad (1)$$

Where

$V_d$  = full scale input voltage range (from amplifier if used) = 10V

$V_d$  = full scale output voltage range = 20V

$R$  = resolution required in engineering units

$E$  = engineering unit represented by  $V_s = 10\text{mm}$

$n$  = bit resolution of the ADC

$B = 1$  if bipolar range, 0 if unipolar;  $B = 1$  for this case

Thus it was then decided to use ADC resolution of 14 bits. Back calculated from above equation the resolution is 0.00061mm which is equivalent to 0.00094% of strain. Because of other considerations, however, such as environmental noise (cell phones particularly introduce radio frequency noise) as well as noise within the signal conditioning system, this theoretical resolution is rarely attainable.

The applied load on the sample was recorded by a submersible load cell (2kN capacity) positioned above the top platen of the specimen inside the Perspex cylinder so that the recorded data was unaffected by any inevitable frictional forces. The load cell is manufactured by GDS with an accuracy of  $\pm 0.1\%$  of total capacity i.e.  $\pm 2\text{N}$ . Thus for a sample with diameter of 50mm the accuracy is within 1kPa.

The cell pressure was applied by water pressure using de-aired water by a GDS Digital Pressure Volume Controller (DPVC). A DPVC is a microprocessor controlled linear actuator for precise regulation and measurement of liquid pressure and liquid volume change. It can be directly connected to a computer for computer control via a General Purpose Interface Bus (GPIB).

Internal back pressure was recorded at the top of the specimen and a secondary independent pore pressure transducer located at the bottom platen of the specimen. Figure 2 shows an overview of the apparatus used in this study. Three tests that were conducted following  $K_0$  consolidation of loose soil are the focus of this paper.

### 2.3 Sample reconstitution

Several methods for preparing reconstituted silty sand in the laboratory have been reported in the literature. The two most common methods are moist tamping (Ladd, 1978) and dry pluviation (Bahadori *et al.*, 2008; Ishihara, 1993; Sitharam & Dash, 2008; Yamamuro & Wood, 2004). Dry pluviation produce fabric which is similar to natural fabric deposition (Jang & Frost, 1998; Oda *et al.*, 1978). Moist tamping produces a consistent preparation method and avoids segregation problems (particularly for silty sand as used in this study). It is also found to give a good control over the global specimen density. While moist tamping does not replicate natural deposition, maintaining a consistent preparation method throughout testing ensured that all results were equally affected by the preparation method. Aging can be manifested in samples prepared by both methods (Yusa, 2015). This paper focuses therefore on aging of moist tamped samples.

For moist tamped samples, a predetermined amount of water was added to give 10% moisture content so that particles would adhere slightly through capillary suction. Then the moist soil was put into the split mould, layer by layer and tamped slightly to a predetermined height using the under-compaction method. In this way good control of the soil density was ensured. Detail of the method can be read on the paper by Ladd (1978).

Loose samples were reconstituted to a relative density of 39.6%  $\pm$  0.3%. Table 1 shows the test program in this study.

Table 1 Test program

No	Dr (%)	$\sigma'_3$ (kPa)	$K_0$	Test ID
1	39.4	120	0.46	CKoU-15
2	39.6	60	0.48	CKoU-18
3	39.9	30	0.52	CKoU-21

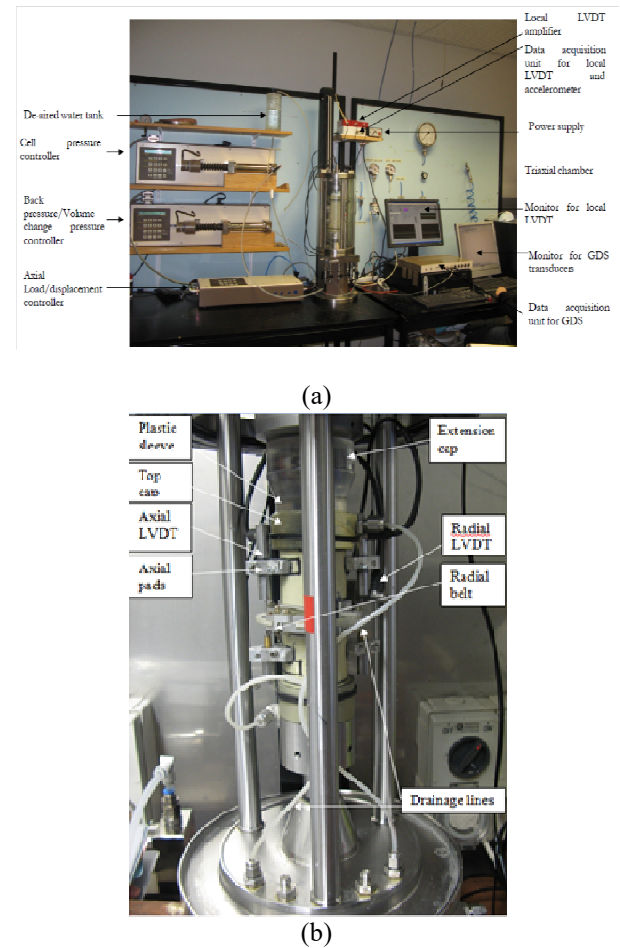


Fig. 2 Overview of the triaxial apparatus (a) and sample setup (b)

### 2.4 Saturation and $CO_2$ percolation

During preparation of on-sample instrumentation the sample was held under 15 kPa of suction, which was then replaced by 15 kPa of cell pressure. The samples were then saturated by slowly percolating  $CO_2$  for 1.5

hours (2-3 air bubbles per second) under the same cell pressure, followed by water under 0.3m head to minimize loss of fines. A saturation B value > 0.98 was obtained for all the samples.

## 2.5 $K_0$ consolidation

The  $K_0$  module program developed by GDS was used to perform  $K_0$  consolidation. There are two methods to maintain zero lateral strain, either direct reading of the specimen diameter or using the volume change calculation.  $K_0$  using direct reading is preferable; however the connection/splitter to tie the GDS data acquisition system and local data was not yet available during the test. Thus throughout this study  $K_0$  consolidation were done based on volume change measurement. During  $K_0$  consolidation, external axial displacement is adjusted slowly thus ensuring the diameter of the specimen remains constant, where the specimen diameter change is theoretically calculated from the back pressure volume change. The required inputs of this program module were the target confining and back pressures and the time to reach the target. The module increases them simultaneously at a certain loading rate. Trials were performed to choose a suitable loading rate which, in this study, was 15kPa/hour. This rate is considered reasonably slow enough to allow the sample to fully consolidate during loading, and no significant change in pore water pressure was observed during  $K_0$  loading. In this study, consolidation is considered to be finish if no excess pore pressure was generated when the target consolidation stress is reached. Similar consideration was used by previous studies (e.g. Bowman, 2002; Lam, 2003)

In this study, the state of stress is described using “Cambridge q-p’ “stress invariants.

Deviator stress is defined as

$$q = (\sigma'_1 - \sigma'_3) \quad (2)$$

Mean effective stress is defined as

$$p' = \frac{1}{3} (\sigma'_1 + 2\sigma'_3) \quad (3)$$

where  $\sigma'_1$  and  $\sigma'_3$  are major and minor principal stresses.

## 2.6 Creep

Following the consolidation stage, a creep stage was performed by targeting constant cell pressure, back pressure and deviator stress for

certain periods of creep – i.e. one week. It was important that these stresses during creep were reasonably stable i.e. within  $\pm 1$ kPa of the target value

Local strains are presented in terms of calculated volumetric and shear strain data along with the measured axial and radial strain. Local volumetric strain is defined as

$$\varepsilon_v = \varepsilon_a + 2\varepsilon_r \quad (4)$$

Shear strain is defined as

$$\varepsilon_s = 2/3(\varepsilon_a - \varepsilon_r) \quad (5)$$

## 3 RESULTS AND DISCUSSION

Fig. 3 and Fig. 4 show strain and stress paths respectively during  $K_0$  consolidation i.e. for 120 kPa (CKoU-14), 60 kPa (CKoU-17) and 30 kPa (CKoU-20) confining pressure. Fig. 3 demonstrates, as expected for  $K_0$  consolidation, the slope of the local strain path is equal to unity for all confining pressures as the radial strains are zero. The same figure also shows that the axial strain developed during  $K_0$  consolidation is greater for higher confining pressure. It can be seen from Fig. 4 that the stress paths for three confining pressures appear to be almost on top of each other. Further observation reveals that the stress paths are slightly different. Higher confining pressure during  $K_0$  consolidation results in a slightly less steep gradient. This is due to the fact that the  $K_0$  value ( $=\sigma'_3/\sigma'_1$ ) is decreasing as mean effective stress increases and practically reaches a constant value when the mean effective stress is higher than 100kPa. Okochi and Tatsuoka (1984) found a similar trend. As a result, each end point for a different confining pressure has a different stress ratio,  $R$  ( $=1/K_0$ ), and effective mean stress ( $p'$ ). This may be due to different between the stress ratio at the initial isotropic stress condition ( $R=1$ ) and the stress ratio when  $K_0$  reach the ultimate value. Okochi and Tatsuoka (1984) reported that when  $K_0$  value at relatively low confining pressure to be determined accurately, the initial stress ratio should be close to ultimate  $K_0$  value. Thus when comparing creep at different confining pressures for each density, we are actually comparing creep due to the combined effects of stress ratio and mean effective stress.

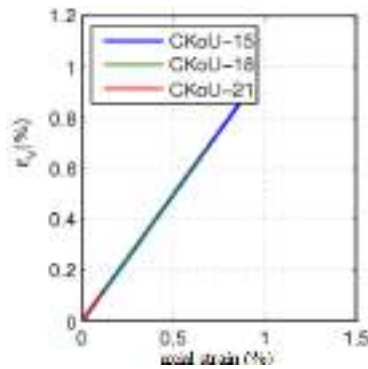


Fig. 3 Strain path during consolidation

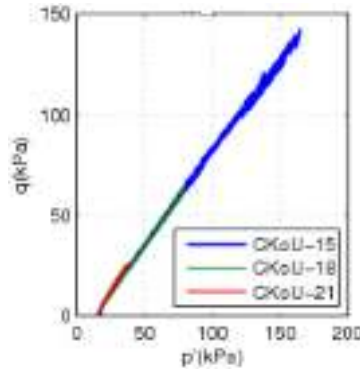


Fig. 4 Stress path during consolidation

Fig. 5 illustrates the combined effect of confining pressure and stress ratio on development of creep strain of loose samples at 120 kPa (left), 60 kPa (middle) and 30 kPa (right) confining pressure, respectively. Fig. 5 (a) to Fig. 5(c) shows that axial strain increases in compression with time at a decreasing strain rate for all confining pressure samples. This is in accordance to Shozen (2001) and Lam (2003) who performed aging tests on loose clean Fraser River sand. The same figures also show that axial strain tends to be greater at higher confining pressure. Fig. 5(d) to Fig. 5(f) generally show radial strain generally is generally negligible. Despite of that there is a slight tendency of increasing negative radial strain which indicate some degree of radial expansion. In terms of volumetric strain development, loose samples up to one week of aging contract / compress during creep with greater confining pressure result in larger volumetric strain as shown by Fig. 5(g) to Fig. 5(i). Similar contraction trend in term volumetric strain was also observed (based on volume change) by previous researchers (Lade *et al.*, 2009; Lam, 2003; Shozen, 2001) who studied aging of loose clean sand. This similar trend could be related to due fact that the behaviour of the 15% fine silty sand is still sand dominated. Discrete element modelling studies (e.g. Kang

*et al.*, 2012; Suarez *et al.*, 2009) also confirmed the contraction trend of loose samples during creep. Shear strains i.e. Fig. 5 (j) to Fig. 5 (h) respectively, suggest that are in the positive direction. This was expected due to greater axial stress than radial stress when the creep starts.

#### 4 SUMMARY

This study has shown that during creep loose silty sand with 15% fine content in this study is contractive. During creep the amount of radial deformation is very small compare to axial strain with tendency of radial expansion.  $K_0$  condition before creep stages results in shear. Additionally this study also shows that creep strain is larger for higher confining pressure.

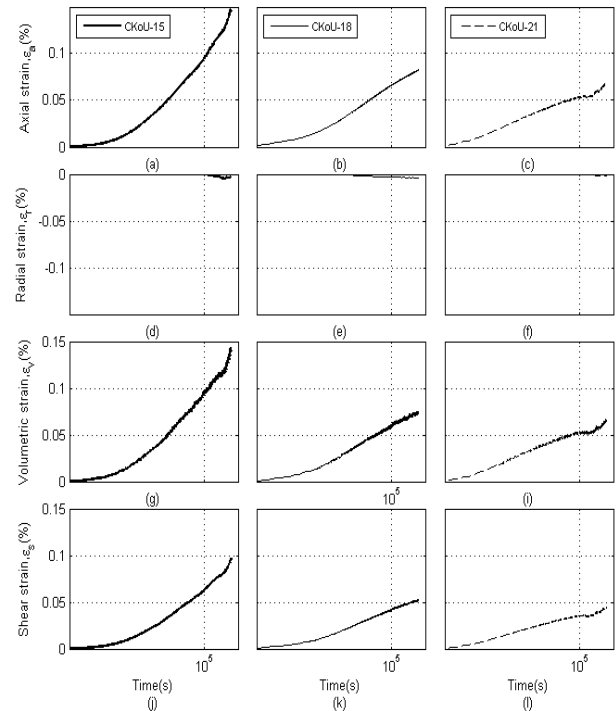


Fig. 5 Creep strains

#### ACKNOWLEDGEMENTS

This research was made possible with funding from Earthquake Commission (EQC) Capability Research Funding Project Scholarship New Zealand.



## REFERENCES

- Bahadori, H., Ghalandarzadeh, A., & Towhata, I. (2008). Effect of non plastic silt on the anisotropic behavior of sand. *Soils and Foundations*, 48(4), 531-545.
- Bowman, E. T. (2002). *The Ageing and Creep of Dense Granular Materials*. PhD Thesis, University of Cambridge, Cambridge, UK.
- Cubrinovski, M. (2013, 29 April-4 May). *Liquefaction-Induced Damage in 2010-2011 Christchurch (New Zealand) Earthquakes*. Paper presented at the 7th International Conference on Case Histories in Geotechnical Engineering, Chicago, Illinois-USA.
- Howie, J., Shozen, T., & Vaid, Y. (2002). Effect of ageing on stiffness of very loose sand. *Canadian Geotechnical Journal*, 39(1), 149-156.
- Ishihara, K. (1993). Liquefaction and Flow Failure during Earthquakes. *Geotechnique*, Vol. 63, 351 - 415.
- Jang, D. J., & Frost, J. D. (1998). *Sand Structures Differences resulting from Specimen Preparation procedures*. Paper presented at the ASCE Specialty Conference on Geotechnical Earthquake Engineering and Soil Dynamic, Seattle.
- Kang, D. H., Yun, T. S., Lau, Y. M., & Wang, Y. H. (2012). DEM simulation on soil creep and associated evolution of pore characteristics. *Computers and Geotechnics*, 39(0), 98-106. doi: 10.1016/j.compgeo.2011.09.003
- Kuwano, R., & Jardine, R. J. (2002). On measuring creep behaviour in granular materials through triaxial testing. *Canadian Geotechnical Journal*, 39(5), 1061-1074.
- Ladd, R. (1978). Preparing Test Specimens Using Undercompaction. *ASTM Geotechnical Testing Journal*, Vol. 1(1), 16-23.
- Lade, P. V. (1994). Creep effects on static and cyclic instability of granular soils. *Journal of Geotechnical Engineering - ASCE*, 120(2), 404-419.
- Lade, P. V., Liggio, C. D., & Nam, J. (2009). Strain rate, creep, and stress drop-creep experiments on crushed coral sand. *Journal of Geotechnical and Geoenvironmental Engineering*, 135(7), 941-953.
- Lam, C. K. K. (2003). *Effects of Aging Duration, Stress Ratio during Aging and Stress Path on Stress-Strain Behaviour of Loose Fraser River Sand*. MASc, University of British Columbia.
- Mitchell, J. K. (2008). *Aging of Sand- A Continuing Enigma?* Paper presented at the 6th Int. Conf. on Case Histories in Geotechnical Engineering, Arlington, VA.
- Oda, M., Koishikawa, I., & Higuchi, T. (1978). Experimental study of anisotropic shear strength of sand by plane strain test. *Soils and Foundations*, 18(1), 25-28.
- Okochi, Y., & Tatsuoka, F. (1984). Some factors affecting Ko-values of sand measured in triaxial cell. *Soils and Foundations*, 24(3), 52-68.
- Schmertmann, J. H. (1991). The Mechanical Aging of Soils. *Journal of Geotechnical Engineering*, 117(9), 1288-1330.
- Shozen, T. (2001). *Deformation under the constant stress state and its effect on stress-strain behaviour of Fraser River Sand*. Master of Applied Science, University of British Columbia.
- Sitharam, T., & Dash, H. (2008). Effect of Non-Plastic Fines on Cyclic Behaviour of Sandy Soils *GeoCongress 2008 : Geosustainability and Geohazard Mitigation* (pp. 319-326).
- Suarez, N. R., Brandon, L., & Mitchell, J. K. (2009). Discrete Element Modeling of Aging in Granular Media. In H. I. Ling, A. Smyth & R. Betti (Eds.), *Poromechanics IV* (pp. 335-340). Lancaster: DEStech Publications, Inc.
- Taylor, M. L., Cubrinovski, M., & Haycock, I. (2012). *Application of new 'Gel-push' sampling procedure to obtain high quality laboratory test data for advanced geotechnical analyses*.
- Wang, Y.-H., & Tsui, K.-Y. (2009). Experimental Characterization of Dynamic Property Changes in Aged Sands. *Journal of Geotechnical and Geoenvironmental Engineering*, 135(2), 259-270. doi: 10.1061/(asce)1090-0241(2009)135:2(259)
- Yamamuro, J. A., & Wood, F. M. (2004). Effect of depositional method on the undrained behavior and microstructure of sand with silt. *Soil Dynamics and Earthquake Engineering*, 24(9-10), 751-760. doi: 10.1016/j.soildyn.2004.06.004
- Yusa, M. (2015). *Aging and Creep of Non Plastic Silty Sand*. PhD, University of Canterbury, Christchurch.